Piezoelectric Active-Sensor Diagnostics and Validation using Instantaneous Baseline Data

Timothy G. Overly, Gyuhae Park, Kevin M. Farinholt, Charles R. Farrar

***Abstract*— This paper presents a signal processing tool that efficiently performs piezoelectric sensor diagnostic and validation. Validation of the sensor/actuator functionality during structural health monitoring (SHM) operation is a critical component to successfully implement a complete and robust SHM system, especially with an array of piezoelectric (PZT) active-sensors involved. The basis of this method is to track the capacitive value of PZT transducers, which manifests in the imaginary part of the measured electrical admittance. Both degradation of the mechanical/electrical properties of a PZT transducer and the bonding defects between a PZT patch and a host structure can be identified by the proposed process. However, it is found that temperature variations in sensor boundary conditions manifest themselves in similar ways in the measured electrical admittances. Therefore, we examine the effects of temperature variation on the sensor diagnostic process and develop an efficient signal processing tool that enables the identification of a sensor validation feature that can be obtained instantaneously without relying on pre-stored baselines. The paper concludes with experimental results to demonstrate the effectiveness of the proposed technique.**

***Index Terms*— Active-Sensing, Piezoelectric Transducers, Sensor validation, Structural Health Monitoring,**

I. Introduction

Structural health monitoring (SHM) techniques based on the use of active-sensing piezoelectric materials have received considerable attention in the structural community. A key component to any successful active-sensing SHM system is the ability to assess the condition of sensors and actuators installed on the structure being monitored, as sensor/actuator malfunction is a major source of failure in SHM systems. Sensor/actuator fracture is the most common type of transducer failure, which can be attributed to the brittle nature of many piezoelectric (PZT) devices. Additionally, maintaining sufficient bonding conditions between a transducer and a host structure over the long service life of many SHM systems can be difficult. Changes in bonding condition or degradation of the mechanical/electrical properties of the transducer could cause false damage identification, compromising the ability of SHM systems to accurately evaluate the condition of the host structure.

It has been pointed out by Friswell and Inman [1] that the field of sensor validation has received very little attention in the structural dynamics community as compared to the process control of chemical engineering. Here, sensor validation refers to the capability of detecting and isolating a faulty sensor in a sensing network. Subsequently, they propose a sensor validation method based on the comparison between a subspace of the response and a subspace generated by the lower structural modes. Their method was further extended by generating new residuals using the modal filtering approaches [2]. Worden used auto-associative neural networks and principal component analysis (PCA) to identify errant sensors [3]. Kerschen et al. [4] present a procedure based on PCA, which is further able to perform detection, isolation, and reconstruction of a faulty sensor. However, the aforementioned studies are usually limited to those sensors used for measuring lower-order vibrational modes and are not usually able to discriminate the changes associated with a sensor fault from those of structural changes.

Methods for specifically determining the health of piezoelectric (PZT) patches have also been examined in previous research. A couple of the techniques specifically make use of the impedance measurements of the piezoelectric patch. Saint-Pierre et al. [5] use the shape of the first real impedance resonance and its change to determine the state of the bonding condition. Guirgiutiu and Zagrai [6] propose a similar technique using the attenuation of the first imaginary impedance resonance for sensor debonding detection. Pacou et al. [7] discuss the use of a shift in the first natural frequency of the piezoelectric patch before and after bonding as a possible method for determining bonding condition. These methods however require a high-frequency data-acquisition system because the first resonance of PZT wafers in SHM applications is usually found in the hundreds of kHz range. In addition, these methods are not able to account for sensor fracture, which can simultaneously occur with de-bonding, as the sensor breakage would apparently change the resonant frequencies of a PZT sensor. Bhalla and Soh [8] investigate the effect of the shear lag loss on electromechanical impedance measurements. They suggest that the imaginary part of the electrical admittance of PZT transducers may play a meaningful role in detecting deterioration of the bond layer.

Manuscript received May 9, 2008.

T. G. Overly is with the Los Alamos National Laboratory, Los Alamos, NM 87545 USA (email: toverly@lanl.gov).

G. Park is with Los Alamos National Laboratory, Los Alamos, NM 87545 USA (corresponding author, phone: 505-663-5335; fax: 505-663-52255; e-mail: gpark@lanl.gov)

K. M. Farinholt is with the Los Alamos National Laboratory, Los Alamos, NM 87545 USA (email: farinholt@lanl.gov).

C. R. Farrar is with Los Alamos National Laboratory, Los Alamos, NM 87545 (email: farrar@lanl.gov).

However, by concentrating on the effects of bond layers on the electromechanical impedance spectrums, the metrics that can be used for bond quality assessment were not clearly identified, and the ability to discriminate bond failures from structural damage was not thoroughly investigated. Recently, the authors propose a sensor diagnostic process that tracks changes in the capacitive value of PZT transducers [9]. Both the degradation of the mechanical/electrical properties of a PZT transducer and the bonding defects between a PZT patch and its host structure can be identified by the process. This method is also able to distinguish response changes caused by sensor failure from those caused by structural damage. The authors further investigated the effects of sensor/structure bonding defects on high frequency SHM techniques, including Lamb wave propagations and impedance methods. It has been found that the effects are significant, modifying the phase, amplitude, and shape of propagated Lamb waves and changing the measured impedance spectrum, which could lead to false indications on structural conditions [10].

The primary goal of this paper is to present an efficient signal processing tool that can be used for sensor diagnostics and validation for PZT transducers used in SHM applications. This signal processing tool is based on the authors' previous development in PZT sensor diagnostics and validation processes [9,10]. In the previous work it was found that temperature variations and changes in sensor boundary conditions could manifest themselves in the measured electrical admittances in a way that was difficult to distinguish from sensor defects. Therefore, in this paper, we examine the effects of temperature variation on the sensor diagnostic process. We then classified several key characteristics of temperature change and developed an efficient signal processing technique to account for those variations in the sensor diagnosis process. This proposed method will be very effective in providing a metric that can be used to determine the sensor functionality over a long period of time. The proposed procedure can also be useful if one needs to check the operational status of a sensing network right after its installation.

The rest of this paper includes a brief description of the proposed sensor diagnostic method, the temperature effects on the diagnostic process, a signal processing toolset, and experimental procedures and results to verify the proposed signal proceeding technique.

II. Piezoelectric Sensor Diagnostic and Validaton Process

The sensor diagnostics and validation process is based upon the capabilities demonstrated in the previous studies of the impedance-based structural health monitoring method [11,12,13,14]. The basic concept of the impedance method is to use high frequency vibrations to monitor the local area of a structure for changes in structural impedance that would indicate damage or imminent damage. This process is possible using piezoelectric sensor/actuators whose electrical impedance is directly related to the structure's mechanical impedance. The impedance measurements can easily give information on changing parameters, such as resonant frequencies or damping, which allows for the detection and location of damage. The expression for the one-dimensional electromechanical admittance ($Y(\omega)$) of a PZT transducer, which is bonded to a structure, is given in Equation (1) [15],

$$Y(\omega) = i\omega \frac{wl}{t_c}\left(\varepsilon_{33}^{T}(1-i\delta) - d_{31}^{2}Y_p^E + \frac{Z_a(\omega)}{Z_a(\omega)+Z_s(\omega)} d_{31}^{2}\hat{Y}_p^E\left(\frac{\tan kl}{kl}\right)\right) \quad (1)$$

where w, l, and h are width, length, and height of the PZT patch, respectively, $Z_s(\omega)$ and $Z_a(\omega)$ are the mechanical impedance of the host structure and of the PZT transducer respectively, Y_p^E is the complex Young's modulus of the PZT patch at zero electric field, d_{31} is the piezoelectric constant and ε_{33} is the dielectric constant of the PZT wafer. The wave number of the PZT patch, k, is defined as,

$$k = \omega\sqrt{\frac{\rho}{\hat{Y}_p^E}} \quad (2)$$

where ρ is the mass density of the PZT material. Equation (1) is derived based on an assumption that a PZT patch is attached to one end of a structural system, whereas the other end of the PZT is fixed. This assumption regarding the interaction at two discrete points is consistent with the mechanism of force transfer from the bonded PZT transducer to the structure.

Equation (1) sets the groundwork for using PZT active-sensors for impedance-based structural health monitoring applications. Assuming that the mechanical and electrical properties of the PZT patch do not change over the monitoring period of a host structure, Equation (1) clearly indicates that the electrical admittance (or impedance) of the PZT wafer is directly related to the mechanical impedance of the host structure, allowing for monitoring of the host structure's mechanical properties using the measured electrical property.

On the other hand, the electrical admittance of a PZT transducer under a free-free boundary condition is given in the following relationship [16],

$$Y_{free}(\omega) = i\omega\frac{wl}{t_c}\left(\varepsilon_{33}^{T}(1-i\delta)\right) \quad (3)$$

The sensor diagnostic process [9,10] is based on Equations (1) and (3). The electrical admittance is clearly a function of the geometric constants (w, l, t_c), mechanical properties (Y_p^E), and electrical properties (ε_{33}^{T}, d_{31}, δ) of a PZT transducer. It is also obvious from the equations that changes in these properties are manifested more distinctly in the imaginary part of the electrical admittance. Therefore, breakage of the sensor and degradation of the sensor's quality can be identified by monitoring the imaginary part of the electrical admittance. The breakage/degradation of the sensor quality would cause a

downward shift in the slope of the admittance, as the effective size of the sensor would decrease with the breakage and the values of dielectric constants and piezoelectric coupling constants would decrease with degradation. The slope of the admittance is analogous to the capacitive value of the PZT material.

Another significant observation that can be made from equations (1) and (3) is that one can identify the effect of the bonding layer on the measured electrical admittance. The effect of the bonding layer is obtained by assuming the mechanical impedance of a structure is much greater than that of the piezoelectric transducer in Eq. (1), which makes the last term in Eq. (1) close to zero, simplifying it to,

$$Y_b(\omega) = i\omega \frac{wl}{t_c}\left(\varepsilon_{33}^{T}(1-i\delta) - d_{31}^{2}Y_p^E\right) = Y_{free}(\omega) - i\omega\frac{wl}{t_c}\left(d_{31}^{2}Y_p^E\right) \quad (4)$$

It is clear from Eqs. (3) and (4) that the electrical admittance of the same PZT patch is different if under a free-free condition or surface-bonded (or commonly referred to as blocked) condition. The blocked condition would cause a downward shift in the slope of the electrical admittance (decrease in the capacitive value) of a free PZT by a factor of $(wl/t_c)d_{31}^{2}Y_p^E$. The assumption that leads to this result is valid, especially at a lower frequency range, because the mechanical impedance of the structure is usually several orders of magnitude greater than that of a PZT transducer. Even though this derivation does not explicitly consider the parameters of bonding materials (such as thickness or shear modulus), it is obvious from Equation (4) that the use of a PZT transducer with lower Y_p^E and a smaller dimension, such as a small PVDF patch, will reduce the effect of the bonding layer on the measured admittance, which is consistent with the shear-lag analysis available in the literature [8,17]. This analysis is also consistent with the definition of the electromechanical coupling coefficient, which is a fraction of the input electrical energy that is mechanically deliverable, or vise versa [18]. In short, the importance of Eq. (4) is that the bonding layer also contributes to the overall admittance of PZT patches bonded to a structure. Thus, bonding defects would also affect the measured admittance. Contrary to sensor breakage, bonding defects would cause an upward shift in the slope of the imaginary part of the electrical admittance (decrease in the capacitive value). Therefore, sensor functionality including sensor breakage and degradation of the bonding condition can be assessed by monitoring the imaginary part of the admittances. A detailed explanation of the sensor diagnostic technique used and the mathematical derivations supporting this can be found in the authors' previous work [9,10].

III. Experimental Investigation of Sensor Diagnostic and Validation Process

For the sake of completeness, some experimental results of the sensor diagnostic process are briefly presented. Various types of sensor failure will affect the imaginary admittance in different ways. The first step in the diagnostic process is to quantify those changes for different bonding and sensor-faulty conditions. This classification will allow the imaginary admittance measurements to be used in a meaningful way in a sensor diagnostic procedure. The two main types of sensor failure being examined are sensor debonding and sensor breakage.

A. Debonding

Sensor debonding is a failure mode of considerable concern, because, unlike some of the other failure modes, it is not readily noticeable upon visual inspection. Debonding may occur in a situation where the structure may not have sustained any damage, i.e. a large strain for the PZT but within the operating parameters of the structure, an impact loading on the structure by foreign objects, or the long-term degradation of the adhesive bond.

To illustrate the effects of debonding, nine circular PZT patches (12.7 mm diameter) were bonded using super glue to a 6.35 mm thick aluminum plate. In this testing, three were bonded fully, three were bonded with 25 percent debonding, and the remaining three were bonded at 50 percent. To implement the partially bonded samples release paper was used to restrict adhesion to only the desired contract regions. Specifically, the PZT was bonded to the plate with a corresponding percent of the total area separated by a double layer of release paper. Figure 1 shows the experimental condition of the bonded sensors.

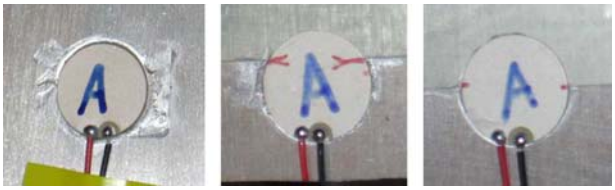

(a) 0 % (b) 25% (c) 50%

Figure 1: Various debonding percentages on PZT patches

As stated before, the debonding of sensors has an effect on the sensor diagnostic indicator that we are examining, specifically the imaginary part of the admittance (susceptance). For this indicator the slope changes in a repeatable and consistent manner with debonding percentages.

Figure 2 shows that the slope of the susceptance decreases with debonding. It can also be seen in the graph that there is a progression of measurements from the highest slope, a reference free-free set, to the lowest slope, the fully bonded case. This decrease is consistent with a previous study [9], but this investigation shows that the percent of change is also proportional to the amount of debonding.

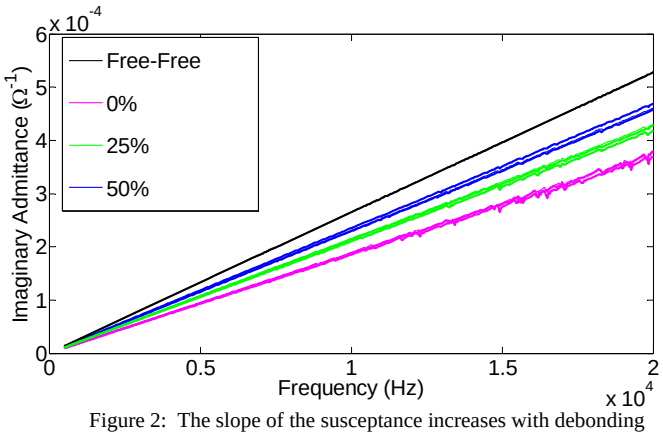

Figure 2: The slope of the susceptance increases with debonding percentage

B. *Breakage*

The second sensor failure mode to be investigated is sensor breakage. Over a long service life or after an impact on the structure by foreign objects, it is possible that the PZT sensor has been damaged, causing a potentially erroneous measurement of the structure. To investigate the effects of such an occurrence, six circular PZT patches (12.7 mm diameter) were bonded to a 6.35mm thick aluminum plate and were broken and cut at specific percentages of their total surface area, and then impedance measurements were taken. Three patches were broken or cut to reduce the total area by 25 percent, and three patches were broken or cut to reduce the total area by 50 percent. Two of each three were broken with a chisel, to more accurately simulate a real-world damage event. The remaining patches were cut with an abrasive wheel to insure a more accurate reference case. Figure 3(a) shows the 25 percent breakage case, and Figure 3 (b) shows the 50 percent breakage case.

Impedance measurements of the patches were taken before and after breakage, allowing for a comparison of the actual change in capacitance for each sensor. Imaginary admittance measurements were taken of free-free baseline cases, and all the measurements are shown in Figure 4. It can be seen in Figure 4 that the slope of the imaginary admittance is proportional to the breakage percentage. As the breakage percent increases, corresponding decreases in slope were observed. There is some variance in the slopes of each group, which can most likely be attributed to the inconsistent nature of the fractures. Figure 4 shows that the post breakage patch fragments are not a consistent size, they are approximately 25 and 50 percent reductions, but do have some variance. The line with the greatest decrease in slope corresponds to the cut 50 percent patch, which has the smallest final area, demonstrating a further correlation between final patch size and slope.

IV. Effects of Temperature Changes

As temperature changes, the physical properties of the structure, the bonding layer and PZT sensor will also change. Among the temperature dependent property constants of piezoelectric materials, the dielectric constant, ε_{33}^{T}, exhibits most significant effect on electrical impedance [19]. It modifies the first term of Equation (1), the capacitive admittance, causing a shift in the imaginary admittance measurements made in the previous section, which will impose difficulties in the use of the sensor diagnostic process for real world structures. In order to make the sensor diagnosis procedure viable in a real world setting, temperature effects on the susceptance must be understood and the extent of these effects is examined in this section. Both broken and debonded patches were examined for the effect of temperature on the susceptance for each failure mode.

(a) 25 % breakage

(a) 50 % breakage

Figure 3: The PZT patches were broken using both a chisel and an abrasive cutting wheel

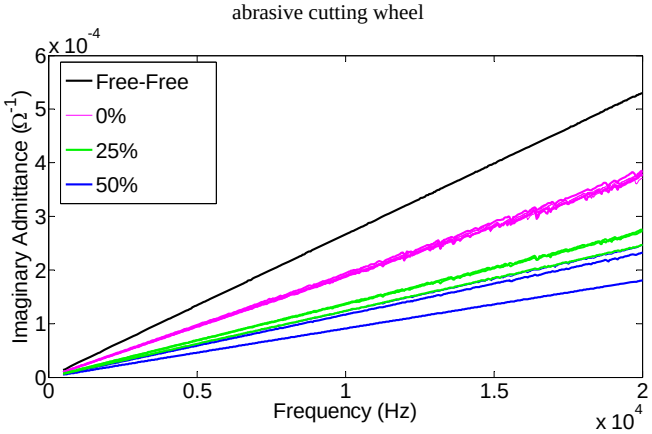

Figure 4: The slope of the imaginary admittance decreases as breakage area increases

A. *Debonding*

The test setup was the same 6.35mm aluminum plate with the debonded patches that was used in the previous section. In addition, the plate was heated and impedance measurements were taken at incremental temperatures. The plate was heated from room temperature to 135 $^{\circ}F$, and the impedance measurements were taken from 500 to 20,000 Hz using an Agilent 4294A impedance analyzer. Once the imaginary admittance measurement was taken at each

temperature, a linear least-squares fit was performed on the measurement to obtain the slope of the signal. This slope value is what was compared from one temperature to the next.

The primary concern was that the slope of the susceptance would vary differently among different bonding and sensor conditions, making it more difficult to assess the bonding condition though the examination of the admittance slope. The results of the temperature test on debonded patches are shown in Figure 5. It can be seen in this graph that as temperature increases, the capacitance value of the PZT increases. Because of the parallel nature of the slope changes, a sensor diagnostic algorithm that is invariant of temperature changes can be developed. If the algorithm uses a system to find outlying PZT sensors, the procedure can be temperature independent, because an outlier will remain an outlier at any temperature, which will be detailed in the next section.

B. Breakage

As an additional check, the effects of temperature on the susceptance measurements of broken patches were also examined. The procedure was the same as the debonding temperature test, but using the broken patches from the previous section. The result of the broken sensor temperature test is shown in Figure 6. As with the debonded sensors, the broken sensors behave in a predictable manner as all the sensor measurements will shift by the same percentage for any given temperature change. The change in both the debonded and broken sensor's susceptance signals indicates however that temperature effects must be removed in a sensor diagnostic algorithm, because sensor failure and temperature changes alter the susceptance signal in a similar manner. The uniform change in various breakage percentages would allow for temperature effects to be removed if a method for outlier detection is used.

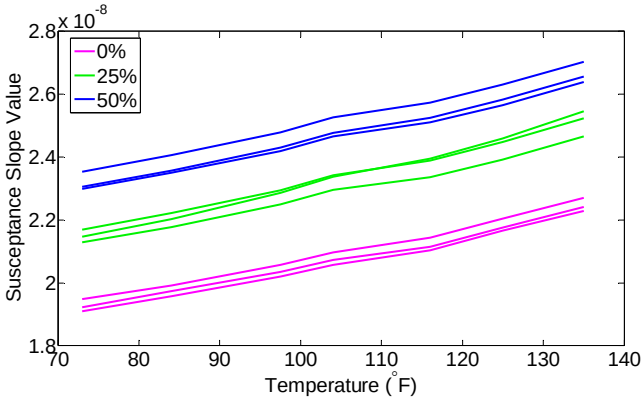

Figure 5: The slope change of susceptance verse temperature for three different bonding percentages

V. Signal Processing for Sensor Diagnostics of Sensor Array

As shown in the previous section, the capacitance of piezoelectric materials is temperature sensitive. Feature identification and signal processing techniques that are able to normalize the measured admittance data with respect to varying environmental conditions are essential if one is to fully apply the proposed sensor diagnostic process under widely varying temperature conditions. Therefore, we developed a procedure that uses the measured admittance values of PZT transducers to allow for the state of the transducers to be obtained without the need for pre-stored baseline measurements. With an array of sensors, this method instantaneously identifies a common feature of healthy sensors and applies a process of outlier detection. Sensors with errant bonding or degraded mechanical/electrical properties could be separated by this process. The method is attractive as an array of sensors is typically deployed in active sensing SHM methods, and these sensors are usually exposed to the same environmental conditions. This procedure is possible because the capacitive value of PZT transducers are predictable with temperature variations (i.e., all the sensors will shift the same percentage for any given temperature change) and one can apply an outlier detection framework at any temperature range, as shown in the previous section.

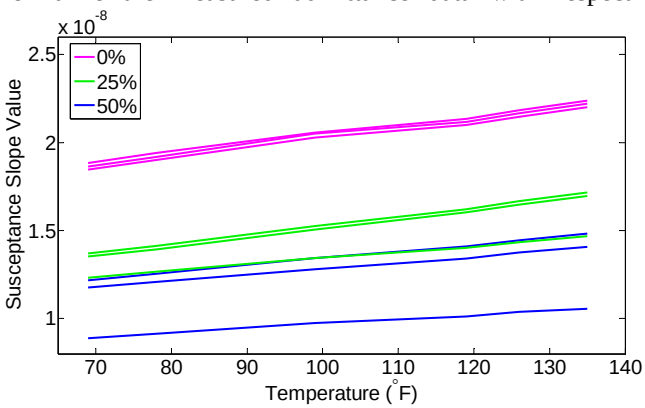

Figure 6: The slope change of susceptance verse temperature for various breakage percentages

The algorithm we developed takes advantage of the characteristic that the removal of an unhealthy patch will cause a greater decrease in the standard deviation of the group of sensors than with the removal of a health sensor. The procedure is,

1. The slope of each of the PZT transducer's admittance signals, which is a measure of the capacitive value, is calculated in a least-squares manner.
2. The transducer in the group that contributes, by its removal, to the maximum reduction in the standard deviation is found.
   (a) One of the PZT transducer's admittance signals is removed and the remaining group's standard deviation is recalculated.
   (b) The PZT transducer with the maximum influence on the standard deviation is recorded and removed from future iterations.
   (c) Steps 2a and 2b are repeated until two sensors remain.
3. The sensors are arranged from the one that has the most influence to the final two sensors. The sensor that corresponds to the maximum distance from the total change

is determined, and is recorded as the sensor that starts the healthy patches. The sensors with a greater influence than this patch are determined to be unhealthy.

A visual representation of the above procedure is shown in Figure 7. The maximum number of recommended unhealthy patches is limited to less than half of the total number of sensors. If a sensor's effect on the standard deviation is negative (it falls above the overall slope change), no sensors are recommended for replacement, because the total slope change does a reasonable job at approximating the individual slope change. It should also be noted that one must use and compare the same size/materials of PZT transducers in order to efficiently use this process and to minimize the variations not related to the sensor conditions.

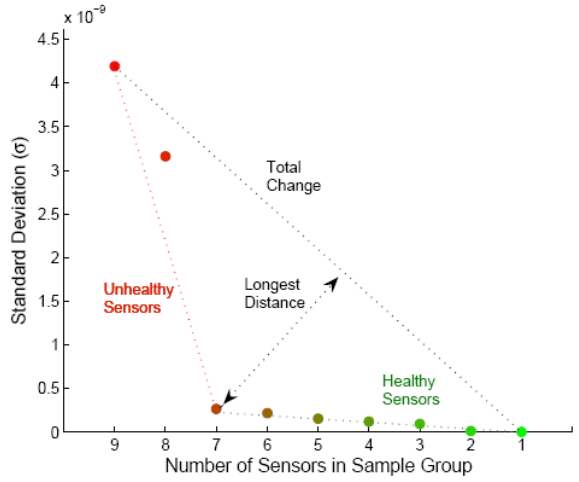

Figure 7: The longest distance form the overall change corresponds to the change from unhealthy to healthy patches

VI. Experimental Verification of the Proposed Signal Processing Tool

Experiments were carried out in order to examine the capability of the proposed method. The first plate was a 1.6 mm thick, solid Aluminum plate that measured 122 x 122 cm. The plate is shown in Figure 8(a) and has very isotropic properties. The second panel tested in this study was a commercially available honeycomb aluminum panel that is composed of two aluminum face sheets bonded to an aluminum honeycomb core. The panel has dimensions 61 x 61 cm with a thickness of 12.7 mm, shown in Figure 8 (b). Each plate had nine PZT sensors (12.7 mm) bounded with varying degrees of health.

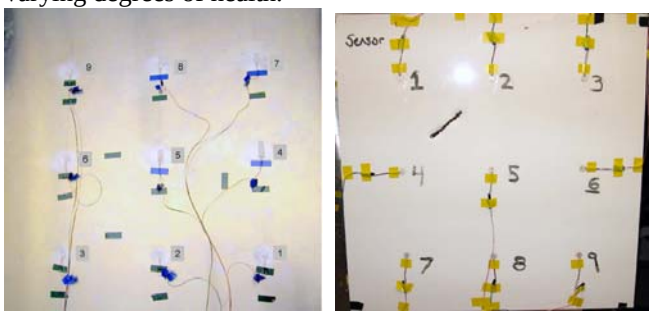

(a) Solid Aluminum Plate (b) Honeycomb Aluminum Plate

Figure 8: Two plates with poorly bonded patches were used to test the sensor array diagnostic algorithm

The sensor diagnostic algorithm was then run on each plate. The output of the proposed algorithm is a hybrid plot with the upper plot showing all of the admittance measurements with color coding corresponding to the lower plot. The lower plot shows the effect of the reducing the sample number with the x-axis showing which sensors are recommended for replacement. The lower plot also has a line delineating the healthy patches from the unhealthy ones. The results from the Aluminum plate are shown in Figure 9 (a), and the results from the honeycomb plate are shown in Figure 10 (a).

When the algorithm was run on each plate, several sensors (sensors 7, 8, 4, 5) on the solid Aluminum plate were recommended for replacement and one sensor (sensor 3) on the honeycomb plate was recommend for replacement. Those sensors were replaced and the algorithm was run again on each plate. Both plates passed the algorithm the second time, as shown in the Figure 9 (b) and Figure 10 (b). It should be noted that the honeycomb plate does have a grouping of values due to the heterogeneous nature of the structure. The grouping of values shows the basic assumption of this sensor validation process, that the structure's impedance is much greater than that of the PZT transducer, does not hold for this structure. In this case, the thinness of the aluminum skin on the plate combined with the relatively stiff honeycomb structure affects the susceptance measurements to a different degree.

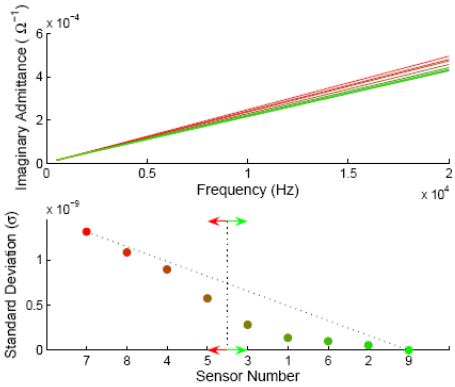

(a) initial condition

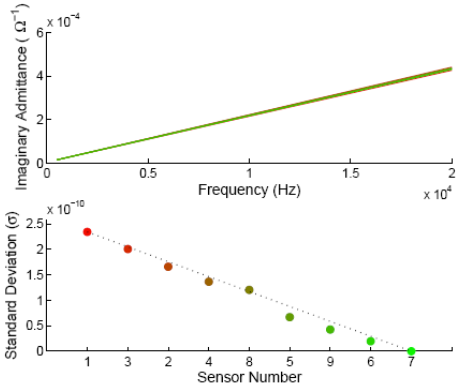

(b) After replacing faulty sensors

Figure 9: The sensor diagnostic process applied to the solid Aluminum plate

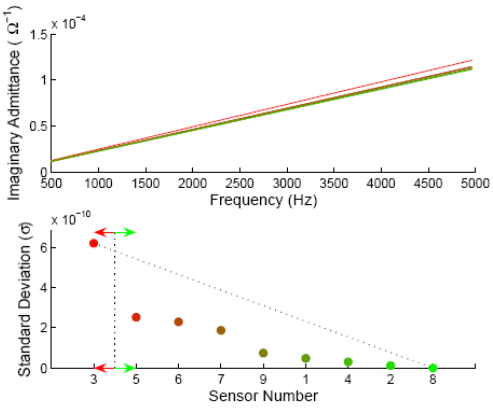

(a) initial condition

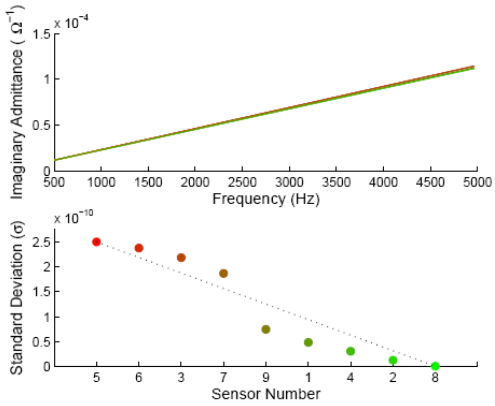

(b) After replacing faulty sensors

Figure 10: The sensor diagnostic process applied to the Honeycomb Aluminum plate

Another test was performed by bonding a faulty sensor on each of the plates at a 50 percent debonded area. The sensors were bonded on each plate at the seven locations, and the partial bonding was introduced using release paper, as discussed in the previous section. Admittance measurements were taken with all the healthy sensors from Figure 9 (b) and Figure 10 (b) except the debonded PZT sensor located at position number seven. The resulting measurements are shown in Figure 11. From the two plots the algorithm correctly identifies the poorly bonded PZT transducers on the solid Aluminum plate and the honeycomb plate.

The main advantage of looking for the change in the data with the proposed algorithm is that no absolute value for the effect of a sensor is required. The lack of a required pre-stored baseline allows this system to be used on a variety of structures with no training set. By instantaneously acquiring a baseline measurement on a structure, we can eliminate the effects of varying environmental conditions and the need to store a pre-recorded baseline. Care does have to be taken to make sure that the sensors being analyzed are exposed to the same environmental conditions, or false positives may occur.

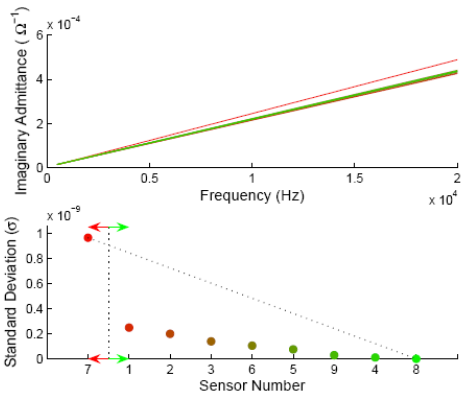

(a) Solid Aluminum Plate

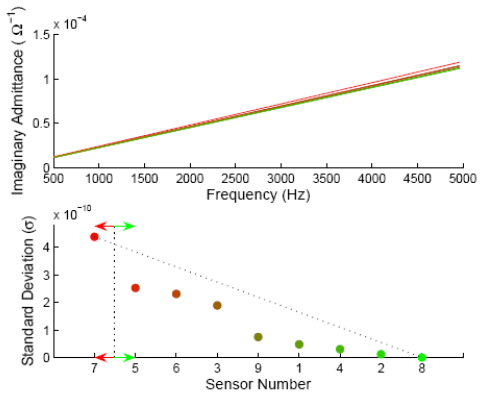

(b) Honeycomb Aluminum Plate

Figure 11: The algorithm correctly identifies the debonded sensor on the solid plate and over estimates the number of damaged sensors on the honeycomb plate.

VII. Conclusion

A piezoelectric sensor self-diagnostic process that performs in-situ monitoring of the operational status of piezoelectric sensors and actuators was presented. It was confirmed that both degradation of the mechanical/electrical properties of a PZT and bonding defects between a PZT and its host structure could be identified using the proposed procedure. The effect of the temperature changes on the sensor diagnostic process was also examined, and was found to be significant. In order to compensate for the effects of temperature changes on the proposed sensor diagnostic process, a rigorous signal processing tool has been developed and experimentally tested for its effectiveness. The method can be readily used with sensor arrays with no pre-stored baseline measurements.

Our current efforts include the development of an improved modeling technique, which incorporates the comprehensive electromechanical effects of the bonding layer on the admittance for more quantitative estimation of the bonding effect, and the search for some other temperature independent features that can be utilized in more rigorous sensor diagnostic process, and these topics will be subjects of subsequent papers.

REFERENCES

[1] M.I. Friswell, D. J. Inman, "Sensor Validation for Smart Structures," *Journal of Intelligent Material Systems and Structures*, Vol. 10, pp. 973-982, 1999.

[2] M. Abdelghani, M. I. Friswell, "Sensor Validation for Structural Systems with Multiplicative Sensor Faults," *Mechanical Systems and Signal Processing,* Vol. 21, No. 1, pp. 270-279, 2007.

[3] K. Worden, "Sensor Validation and Correction using Auto-Associative Neural networks and Principal Component Analysis," *Proceedings of 21st IMAC Structural Dynamics Conference,* Feb 3-6, 2003.

[4] G. Kerschen, P. De Boe, J. Golinval, K. Worden, "Sensor Validation using Principal Component Analysis," *Smart Materials and Structures*, Vol. 14, pp. 36-42, 2005.

[5] N. Saint-Pierre, Y. Jayet, I. Perrissin-Fabert, J. C., Baboux, "The influence of bonding defects on the electric impedance of a piezoelectric embedded element," *Journal of Physics D: Applied Physics*, Vol. 29, No. 12, pp. 2976–2982. 1996.

[6] V. Giurgiutiu, A. N. Zagrai, "Embedded self-sensing piezoelectric active sensors for on-line structural identification," *ASME Journal of Vibration and Acoustics,* Vol. 124, pp. 116–125, 2002.

[7] D. Pacou, M. Pernice, M. Dupont, D. Osmont, "Study of the interaction between bonded piezo-electric devices and plates," *Proceedings, of 1st European Workshop on Structural Health Monitoring,* 2002.

[8] S. Bhalla, C-K. Soh, "Electromechanical impedance modeling for adhesively bonded piezo-transducers," *Journal of Intelligent Material Systems and Structures*, Vol. 15, pp. 955-972, 2004.

[9] G. Park, C. R. Farrar, C. A. Rutherford, A.N. Robertson, "Piezoelectric Active Sensor Self-diagnostics using Electrical Admittance Measurements," *ASME Journal of Vibration and Acoustics,* Vol. 128, No. 4, pp.469-476, 2006.

[10] G. Park, C. R. Farrar, F. Lanza di Scalea, S. Coccia, "Performance Assessment and Validation of Piezoelectric Active Sensors in Structural Health Monitoring," *Smart Materials and Structures*, Vol. 16, No. 6, pp. 1673-1683, 2006.

[11] G. Park, H. Sohn, C.R. Farrar, D.J. Inman, D.J., "Overview of Piezoelectric Impedance-based Health Monitoring and Path Forward," *The Shock and Vibration Digest*, Vol. 35, pp. 451-463, 2003.

[12] V. Giurgiutiu, A. Zagrai, J. J. Bao, "Damage Identification in Aging Aircraft Structures with Piezoelectric Wafer Active Sensors," *Journal of Intelligent Material Systems and Structures*, Vol. 15, pp. 673-688, 2004.

[13] S. Bhalla, C. K. Soh, "High Frequency Piezoelectric Signatures for Diagnosis of Seismic/Blast Induced Structural Damages," *NDT&E International*, Vol. 37, pp. 23-33, 2004.

[14] S. Park, J. J. Lee, C. B. Yun, D. J. Inman, "A built-in active sensing system-based structural health monitoring technique using statistical pattern recognition," *Journal of Mechanical Science and Technology*, Vol. 21, pp. 896-902, 2007

[15] F. P. Sun, Z. Chaudhry, C. Liang, C. A. Rogers, "Truss structure integrity identification using pzt sensor-actuator," *Journal of Intelligent Material Systems and Structures,* Vol. 6, pp. 134–139, 1995.

[16] J. Sirohi, I. Chopra, "Fundamental behavior of piezoceramic sheet actuators," *Journal of Intelligent Material Systems and Structures*, Vol. 11, pp. 47-61, 2000.

[17] J. Sirohi, I. Chopra, "Fundamental Understanding of Piezoelectric Strain Sensors," *Journal of Intelligent Material Systems and Structures*, Vol. 11, pp. 246-257, 2000.

[18] T. Ikeda, *Fundamentals of Piezoelectricity*, 1996, Oxford University Press, Oxford, UK

[19] G. Park, K. Kabeya, H. Cudney, D. J. Inman, "Impedance-based Structural Health Monitoring for Temperature Varying Applications," *JSME International Journal*, Vol. 42, No. 2, pp. 249-258, 1999.

Timothy G. S. Overly Received his MS in Mechanical Engineering from the University of Cincinnati in 2007. While earning his degree, he performed research in the area of structural health monitoring at the Engineering Institute of Los Alamos National Laboratory (LANL). This research included sensor diagnostics, measurement node construction and software development. He is currently working as an analysis engineer and software developer.

Gyuhae Park received his Ph.D. in Mechanical Engineering from Virginia Tech in 2000. He is currently a technical staff member at LANL. He is part of the technical staff of the Engineering Institute, a research and education collaboration between LANL and the University of California at San Diego with a scientific thrust in structural health monitoring and damage prognosis. His recent research focuses on applications and development of active-sensing structural health monitoring, sensor self-diagnostics, and energy harvesting and wireless energy transmission with an emphasis on the use of advanced materials. His research has been documented in over 200 journal articles, conference papers, and book chapters. He is a recipient of the 2007 SHM Person-of-the-Year Award, presented at Stanford University in September 2007.

Kevin M. Farinholt received his Ph.D. in Mechanical Engineering from Virginia Tech in 2005. While a graduate student he served as a National Defense Science and Engineering Graduate Fellow, as well as a Virginia Space Grant Consortium Fellow for his work modeling electroactive polymers. He is currently a postdoctoral research associate at LANL. He is a part of the Engineering Institute, and his research areas include: active material systems, energy harvesting, energy transmission, and structural health monitoring through low-power wireless sensor nodes.

Charles R. Farrar has 25 years experience as a technical staff member, project leader, and team leader at LANL. While at Los Alamos, he earned a Ph. D. in civil engineering from the University of New Mexico in 1988. He is currently the leader of The Engineering Institute at LANL. His research interests focus on developing integrated hardware and software solutions to structural health monitoring problems and the development of damage prognosis technology. The results of this research have been documented in more than 300 publications as well as numerous keynote lectures at international conferences. He is currently working jointly with engineering faculty at University of California, San Diego (UCSD) to develop the LANL/UCSD Engineering Institute with a research focus on Damage Prognosis. His work has been recognized by the Structural Health Monitoring community through the reception of the inaugural Lifetime Achievement Award in Structural Health Monitoring. Additional professional activities the development of a short course entitled *Structural Health Monitoring: A Statistical Pattern Recognition Approach* that has been offered more than 17 times to industry and government agencies in Asia, Australia, Europe and the U.S. He is a Fellow of ASME.